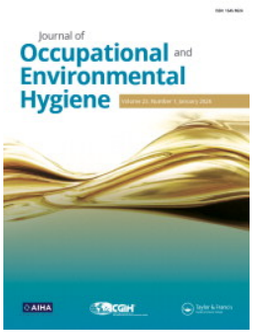

Journal of Occupational and Environmental Hygiene

ISSN: 1545-9624 (Print) 1545-9632 (Online) Journal homepage: www.tandfonline.com/journals/uoeh20

Evaluating the interference potential of minerals in infrared absorbance-based quantification of respirable crystalline silica in mine dusts

David A. Parks, Seth A. Finley, Priscilla M. Tjandra, Leslie L. Baker, Allegra Yeley & Arthur L. Miller

To cite this article: David A. Parks, Seth A. Finley, Priscilla M. Tjandra, Leslie L. Baker, Allegra Yeley & Arthur L. Miller (09 Dec 2025): Evaluating the interference potential of minerals in infrared absorbance-based quantification of respirable crystalline silica in mine dusts, Journal of Occupational and Environmental Hygiene, DOI: 10.1080/15459624.2025.2589136

To link to this article: https://doi.org/10.1080/15459624.2025.2589136

JOURNAL OF OCCUPATIONAL AND ENVIRONMENTAL HYGIENE
https://doi.org/10.1080/15459624.2025.2589136

Evaluating the interference potential of minerals in infrared absorbance-based quantification of respirable crystalline silica in mine dusts

David A. Parks[a], Seth A. Finley[a], Priscilla M. Tjandra[b], Leslie L. Baker[c], Allegra Yeley[a], and Arthur L. Miller[d]

[a]Spokane Mining Research Division, National Institute for Occupational Safety and Health Spokane Mining Research Division Ringgold Standard Institution, Spokane, Washington; [b]University of California San Francisco Ringgold Standard Institution – Orthopaedic Surgery, San Francisco, California; [c]Department of Mathematics and Statistical Science Ringgold Standard Institution – Geological Sciences, University of Idaho, Moscow, Idaho; [d]Miller Consulting United States – Spokane Mining Research Division, Spokane, Washington

ABSTRACT

Miners face a variety of respiratory hazards on the job, including exposure to respirable crystalline silica (RCS), which can lead to adverse health outcomes such as silicosis and lung cancer—both potentially fatal lung diseases. Infrared spectrometry offers the possibility of portable end-of-shift quantification of RCS at mine sites. However, some mine dusts contain minerals that may interfere with this quantification method, as their infrared absorbance bands overlap with those of silica. To evaluate the impact of such interferences, potential mineral interferants were identified in the geologies of 27 metal mines using the United States Geological Survey and Mindat.org databases. These mines were selected based on historically high RCS levels, as evidenced in the Mine Safety and Health Administration (MSHA) field-sampling database, and on the number of employees potentially exposed. The significance of 44 potential interferants was evaluated using Fourier Transform Infrared spectroscopy (FT-IR), by measuring their absorbance per unit mass in the α-quartz doublet region of the spectrum (816–767 cm^{-1}). The extent to which each mineral interfered with this region was quantified as its integrated absorbance relative to RCS. This quantification of interference provides data critical for the timely and portable quantification of RCS in mine dusts. Of the 44 specimens analyzed, three (goethite, azurite and actinolite), which are not mentioned in the standard infrared methods for quantification of RCS, were found to interfere with a magnitude of 10% or more. Despite being commonly mentioned as interferants in the literature, the feldspars Albite and Anorthite did not interfere with a magnitude of 10% or more.

KEYWORDS

Infrared spectrometry; infrared spectroscopy; portable monitor; quartz; real-time monitor; silicosis

Introduction

Miners are at significant risk of overexposure to respirable crystalline silica (RCS), which can lead to a variety of serious health outcomes, including silicosis and cancer (IARC 1997; Straif et al. 2009; Leung et al. 2012; Ehrlich et al. 2021; Misra et al. 2023). Despite extensive understanding of both the causes of and effective prevention strategies for RCS overexposure, workers in many occupational settings continue to experience overexposure (Rice et al. 2001; Martínez et al. 2010; Weissman and Schulte 2011; OSHA/NIOSH 2012; Barnes et al. 2019; Rose 2019; Misra et al. 2023). To address this issue, NIOSH is investigating technologies for real-time and end-of-shift monitoring of RCS, with the goal of improving miner health.

Historically, RCS exposure has been measured using laboratory-based analytical techniques. In non-coal mines, exposure is currently assessed by submitting filter samples, collected with approved respirable samplers, for silica analysis via lab-based X-ray diffraction (XRD). Due to a substantial delay of roughly one week inherent to laboratory analysis, the RCS exposure information can be of limited use for making timely workplace adjustments to reduce exposures. The lack of timely information on exposure underscores the need for the development of field-portable, real-time or end-of-shift methods for RCS monitoring. This study evaluates the efficacy, as it is affected by

CONTACT David A. Parks dparks@cdc.gov Spokane Mining Research Division, National Institute for Occupational Safety and Health Spokane Mining Research Division Ringgold Standard Institution, 315 E. Montgomery Ave., Spokane, WA 99207.

Supplemental data for this article can be accessed online at https://doi.org/10.1080/15459624.2025.2589136. AIHA and ACGIH members may also access supplementary material at http://oeh.tandfonline.com.

mineral interferents, of Fourier Transform Infrared spectrometry (FT-IR) as a viable method for field-portable or end-of-shift RCS quantification in gold, copper, and iron mines. While FT-IR spectrometry is the focus of this work, the findings are also relevant to other infrared absorbance techniques such as diffraction grating spectrometry, quantum cascade laser, and non-dispersive spectrometry.

Mine dust has the potential to contain mineral species that significantly affect the accuracy of RCS quantification via infrared absorbance (Ojima 2003; Ainsworth 2005; Weakley et al. 2014; Miller et al. 2017; Wolfe et al. 2022). Overcoming this obstacle is essential for developing a reliable infrared absorbance-based monitor and is the focus of this study. In this context, an *interferant* is defined as any mineral or compound that produces an infrared response in the same spectral region as the "α-quartz doublet," which consists of two absorbance bands at 780 and 800 cm^{-1}, both associated with Si–O stretching. The 780 cm^{-1} band corresponds to infrared radiation polarized parallel to the crystallographic c-axis, while the 800 cm^{-1} band corresponds to radiation polarized perpendicular to the c-axis (Ocaña et al. 1987). These bands are typically used to calculate an integrated area that correlates with the amount of α-quartz in the infrared beam path. NIOSH methods 7602 SILICA, Respirable Crystalline, by IR (KBr pellet) and 7603 QUARTZ in Respirable Coal Mine Dust, by IR (Redeposition) utilize the 800 cm^{-1} band exclusively (NIOSH 2017a, 2017b) while NIOSH's Field Analysis of Silica Tool (FAST) (Ashley et al. 2020; Chubb and Cauda 2022) the Health and Safety Executive's (HSE) Methods for Determination of Hazardous Substances (MDHS) 101/2 (HSE 2005) uses both bands. For a more complete description of these methods, see Table 1.

While the NIOSH methods 7602 and 7603 and the HSE (MDHS)101/2 involve ashing or digesting the airborne dust collection filter, FAST is conducted directly on a PVC collection filter. Because portable real-time or end-of-shift methods are not compatible with ashing or digesting the collection filter, this study investigates a direct on collection filter approach analogous to FAST methodology.

Previous research has shown that when quantifying RCS in coal mine dust, the interferant spectra introduced by the mineral kaolinite can be corrected using either univariate methods with area ratio correction (Miller et al. 2012) or multivariate methods such as partial least squares regression (Weakley et al. 2014; Miller et al. 2017). While the ability to address kaolinite interference represents a significant advancement in coal mine applications, non-coal mine dusts are often more geologically complex and may contain a wider array of potential interferants, perhaps rendering the former methods ineffective. Notably, a single partial least squares (PLS) regression model was demonstrated to accurately quantify RCS in samples from silver, granite, and limestone mines (Weakley et al. 2014). However, that study did not confirm the presence of mineral interferants beyond calcite, which did not interfere with the α-quartz doublet itself but rather with the kaolinite band used for the kaolinite correction. However, given the definition of granite, it can be inferred that this collection of samples included the often-mentioned potentially interfering minerals of the feldspar group. A separate study using principal component analysis (PCA) on 130 mine samples covering a broader range of mining commodities revealed significant variation in FT-IR spectra and mineral phases—not just between different non-coal mine types, but also within a single mine type (Walker et al. 2021). These findings underscore the need for further investigation into the diverse collection of potential mineral interferants across various mining environments.

The purpose of this study was to (1) generate a list of minerals commonly encountered in the mining environment that may interfere with Si–O vibrational stretching bands and thereby RCS quantification and (2) quantify the extent of these minerals' potential to interfere with the quantification of RCS. In this study, interference was determined by quantifying the apparent "RCS" mass of a respirable sample of a given non-RCS mineral by FT-IR. The apparent "RCS" mass as determined by FT-IR was then ratioed to the gravimetric mass of the same sample. A detailed description of how the interference was quantified is provided in the methods section. In practice, the presence of an interfering mineral biases the RCS quantification proportional to the mass of the interfering mineral within the sample.

The list of potentially interfering minerals is likely extensive, as any mineral possessing a Si–O vibrational stretch may interfere with RCS quantification (ISO 2021). In addition, minerals not possessing a Si–O vibrational stretch can have absorbance bands that incidentally overlap the α-quartz doublet. Adding to the complexity, the term "RCS" refers to three silica polymorphs: α-quartz, tridymite, and cristobalite. This study focuses on α-quartz (also known as low quartz), the most commonly encountered polymorph in

Table 1. Widely used methods for quantifying RCS by way of infrared spectrometry.

Method	Spectrum treatment	Reference
NIOSH Method 7602: SILICA, Respirable Crystalline, by IR (KBr pellet)	Peak amplitude at 800 cm^{-1} after baseline correction	NIOSH 2017a
NIOSH Method 7603: QUARTZ in Respirable Coal Mine Dust, by IR (Redeposition)	Peak amplitude at 800 cm^{-1} after baseline correction	NIOSH 2017b
Health and Safety Executive's (HSE) Methods for Determination of Hazardous Substances (MDHS) 101/2	Peak amplitude at 800 and 780 cm^{-1} after baseline correction	HSE 2005
Field Analysis of Silica Tool (FAST) developed by NIOSH	Integration over 816–767 cm^{-1} after baseline correction	Ashley et al. 2020; Chubb and Cauda 2022

mining environments, and throughout this text, the term RCS is used synonymously with respirable α-quartz.

Methods

Mineral selection

The list of minerals studied was dictated by the mines selected for inclusion in this study. The mines included were those that had airborne RCS concentrations exceeding the MSHA permissible exposure limit (PEL) of 50 $\mu g/m^3$, as documented in the MSHA personal health sample database (MSHA 2024b), and employed more than 200 workers likely to be exposed. A summary of these mines is provided in Table 2. The minerals most frequently listed by the two databases for each commodity are also provided in Table 2. The MSHA employment data considered all employment location subunits within the mine except for office workers in an effort to limit the figures to employees likely to be exposed to RCS.

For these selected mines, geological data were reviewed using two primary databases: United States Geological Survey (USGS) Mineral Resource Data System (MRDS) (https://mrdata.usgs.gov/mrds/) and mindat.org, a self-described "world's largest open database of minerals, rocks, meteorites, and the localities they come from." These databases were used to compile a list of minerals reported in the subset of mines. When possible, the list was limited to minerals accepted by the International Mineralogical Association (IMA) to help ensure that each entry represents a clearly defined mineral with a well-characterized crystalline form (Lafuente et al. 2015). Of the minerals analyzed in this study, all but one (biotite) were IMA-accepted minerals.

Metals or mineraloids such as gold and silver were excluded because they do not exhibit infrared absorbance bands due to the absence of a dipole moment in metallic bonds. While mineraloids do absorb infrared radiation, they do not produce defined absorbance bands in the mid-infrared. As such, baseline correction (as described and illustrated in Figure 1) should mitigate their impact on the quantification of RCS by way of integrating the silica doublet. Conversely, background absorbance is critical in FT-IR analysis, as it is recommended that absorbance values remain within the linear range of 0 to 0.7 absorbance units to avoid nonlinear effects (Griffiths and De Haseth 2007). Further, alternative methods and instrumentation for quantifying α-quartz using infrared absorbance may not benefit from the optical throughput advantage of FT-IR, i.e., Jacquinot's advantage, and the upper limit on absorbance may be considerably lower.

The potential of a given mineral to interfere was preliminarily evaluated by querying two FT-IR spectral databases to determine whether these minerals exhibited known absorbance bands within or near the α-quartz doublet region. In this study, a regression model was developed using the doublet integration from 816—767 cm^{-1}. Given that absorbance bands have finite width and FT-IR measurements have finite resolution, the region of interest when examining spectra from the databases was expanded by 50 cm^{-1} on either side of the integration bounds, resulting in a total spectral window of 866–717 cm^{-1}.

The infrared spectral databases used in this study were the *Infrared Spectra of Mineral Species, Extended Library* (Chukanov 2014) and the RRUFF database (Lafuente et al. 2015). The former provides a discrete list of absorbance bands, while the latter contains raw spectra. The raw spectra from RRUFF were processed in MATLAB Version 23.2.0.2459199 (Matlab R2023b Update 5, Natick, MA, USA). If a given mineral had multiple spectra within the RRUFF database, the spectra were trimmed to include only the range of 866–717 cm^{-1} and preprocessed using Standard Normal Variate (SNV) transformation (Barnes et al. 1989). If only a single spectrum was available for a given mineral, there was no need for or way to apply SNV transformation. The spectra were then treated with a Savitzky-Golay 5-point second-order polynomial filter. After these preprocessing techniques, the first derivative zero-crossing was used to determine the presence

Table 2. Average yearly employment data for 27 US mines by commodity and the most frequently occurring minerals therein (MSHA, 2009–2024).

Mine ID	Commodity	# of Employees	Most Frequently Listed non-Quartz Minerals in Commodity
Mine 1	Gold	367	Pyrite
Mine 2	Gold	715	
Mine 3	Gold	642	
Mine 4	Gold	682	
Mine 5	Gold	261	
Mine 6	Gold	551	
Mine 7	Gold	325	
Mine 8	Gold	397	
Mine 9	Gold	251	
Mine 10	Gold	442	
Mine 11	Gold	250	
Mine 12	Copper	2698	Malachite
Mine 13	Copper	499	Molybdenite
Mine 14	Copper	854	Pyrite
Mine 15	Copper	635	Sphalerite
Mine 16	Copper	302	
Mine 17	Copper	323	
Mine 18	Copper	907	
Mine 19	Copper	300	
Mine 20	Iron	735	
Mine 21	Iron	560	Magnetite
Mine 22	Iron	596	Siderite
Mine 23	Iron	313	
Mine 24	Iron	649	
Mine 25	Iron	310	
Mine 26	Iron	322	
Mine 27	Iron	273	

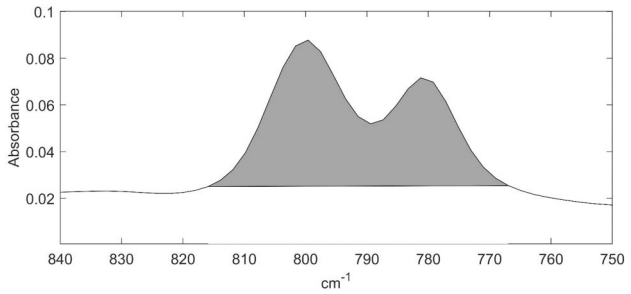

Figure 1. Integration of the quartz doublet. Note the lower limit of the integrated area is defined by a straight line drawn between the absorbances at 816 and 767 cm^{-1}.

and location of any peaks in the doublet region. Lastly, the resulting peak locations were confirmed visually.

Of the 193 minerals reported as present in the 27 mines studied, 59 did not have spectra available in either of the two databases used, nor in other databases which require payment for use, but which provide a public list of the minerals contained therein. This provided yet another motivating factor driving this study. The querying of spectral databases did not inform the selection of minerals to be analyzed, but rather was done so that the correspondence between spectral databases and mineral interference could be evaluated. A perfect correspondence would be highly desirable as it would indicate that querying spectral databases could be sufficient for future evaluation of potential mineral interferants not evaluated in this study.

An effort was made to give priority to obtaining and analyzing the minerals most commonly found in the selected mines. However, this prioritization was somewhat hampered by the restriction to IMA-accepted minerals, which led to the underrepresentation of solid solution minerals. For example, feldspars, the most abundant mineral group in Earth's crust (Neuendorf et al. 2005), are rarely reported as their IMA-accepted pure endmember forms of albite, anorthite, and orthoclase/microcline.

With the compiled list of commonly encountered potentially interfering minerals, these were then sought in their pure form to experimentally assess the degree to which they interfere with RCS quantification via doublet integration of the infrared spectra. Of the 193 minerals considered in this study, only 43 were available for analysis. Given the ubiquitousness of feldspars, multiple attempts were made to procure an orthoclase sample, alas all these were revealed by XRD to be microcline. However, both databases were queried for absorbance peaks in the doublet region for all 193 minerals, and the results are provided in the supplemental material.

Determining mineral content of samples prior to aerosolization

The mineralogical composition of the specimens was determined using powder X-ray diffraction (PXRD), followed by Rietveld refinement (Rietveld 1969) or whole pattern profile fitting (WPF). In cases where specimens produced ambiguous PXRD results, X-ray fluorescence spectroscopy (XRF) was used to aid in the analysis of the PXRD patterns and specification of the specimen's mineralogical composition. The accuracy of PXRD analysis combined with Rietveld refinement for unknown specimens is typically reported to be within ±2–3% (Kaduk 2008). Additionally, in some cases—particularly for minerals identified in this study as interferants the NIOSH Method 7500 Silica, Crystalline, by XRD (filter redeposition) was applied to respirable filter samples to determine the α-quartz content.

In some instances, preferred orientation effects interfered with Rietveld refinement or WPF; these specimens are called out in Table 3 with "preferred orientation" listed in the columns describing

Table 3. List of minerals investigated and their degree of interference.

Primary Mineral	PXRD Intended Mineral (% wt.)	PXRD Quartz (% wt.)	7500 Quartz (% wt.)	Secondary Minerals (% wt.)	Interference (%)	Quartz corrected interference (%)	Baseline [Abs/mg]
Goethite	100	0	Non-detect	0	54	54	0.15
Azurite	98	0	Non-detect	2% Malachite	−24	−24	0.07
Actinolite	60	20	1	2% Chlorite 17% Mica/ Illite	−23	−24	0.07
Microcline	85	0	Not analyzed	15 % Albite	−14	−14	0.12
Kaolinite	Preferred orientation	Preferred orientation	1	Preferred orientation	11	10	Insignificant
Grossular	92	0	Non-detect	8% Diopside	−9	−9	Insignificant
Covellite	96	0	Not analyzed	4% Antlerite	6	6	0.27
Montmorillonite	Preferred orientation	Preferred orientation	Not analyzed	Preferred orientation	5	NA	5
Epidote	100	0	Non-detect	0	−3	−3	Insignificant
Hedenbergite	84	4	Non-detect	5% Monoclinic Amphibole 6% Clay(s)	−3	−3	Insignificant
Malachite	100	0	Non-detect	0	−3	−3	Insignificant
Turquoise	86	7	Not analyzed	4% Illite 3% Pyrite	4	−3[a]	0.07
Muscovite	100	0	Non-detect	0	−2	−2	Insignificant
Galena	100	0	Non-detect	0	1	1	Insignificant
Calcite	98	1	1	1% Dolomite	2	1	Insignificant
Chalcocite	53	4	2	10% Djurleite 1% Hematite, 32% Amorphous	3	1	0.11
Pyrite	100	0	Non-detect	0	−1	−1	0.1
Pyrrhotite	58	0	Not analyzed	41% Troilite 1% Hematite	−1	−1	0.18
Talc	100	0	Not analyzed	0	1	1	Insignificant
Tremolite (monoclinic amphibole)	27	51	13	17% Orthorhombic Amphibole 4% Calcite	13	0	Insignificant
Hematite	100	0	Not analyzed	0	Insignificant	Insignificant	Insignificant
Chamosite	100	0	Non-detect	0	Insignificant	Insignificant	0.1
Anorthite	100	0	1	0	Insignificant	Insignificant	Insignificant
Baryte	100	0	Not analyzed	0	Insignificant	Insignificant	Insignificant
Biotite	100	0	Non-detect	0	Insignificant	Insignificant	Insignificant
Tenorite	87	0	Not analyzed	13% Cuprite	Insignificant	Insignificant	Insignificant
Siderite	100	0	Not analyzed	0	Insignificant	Insignificant	Insignificant
Sphalerite	98	0	Not analyzed	2% Wurtzite	Insignificant	Insignificant	Insignificant
Fluorite	100	0	Not analyzed	0	Insignificant	Insignificant	Insignificant
Albite	100	0	Not analyzed	0	Insignificant	Insignificant	0.03
Cuprite	100	0	Not analyzed	0	Insignificant	Insignificant	Insignificant
Dolomite	99	0	Not analyzed	1% Chalcopyrite	Insignificant	Insignificant	0.05
Enstatite	75	0	Non-detect	18% Feldspar(s) 2% Diopside 5% Talc	Insignificant	Insignificant	Insignificant
Arsenopyrite	100	0	Not analyzed	0	Insignificant	Insignificant	0.08
DPM	Not analyzed	Not analyzed	Not analyzed	not analyzed	Insignificant	Insignificant	0.96
Diopside	92	0	1	5% Magnesiochloritoid 2% Euripium Indium Oxide	Insignificant	Insignificant	Insignificant
Magnetite	60	0	Non-detect	40 % Hematite	Insignificant	Insignificant	0.09
Molybdenite	100	0	Not analyzed	0	Insignificant	Insignificant	Insignificant
Gypsum	100	0	Non-detect	0	Insignificant	Insignificant	Insignificant
Bismuthinite	97	0	Not analyzed	3% Bismuth	Insignificant	Insignificant	Insignificant
Chalcopyrite	97	0	Non-detect	3% Pyrite	Insignificant	Insignificant	0.1
Diopside	54	4	Not analyzed	11% Feldspar 3% Mica/ Illite 17% Calcite 11% Monoclinic Amphibole	Insignificant	Insignificant	Insignificant
Cerussite	84	0	Not analyzed	16% Abellaite	Insignificant	Insignificant	Insignificant

[a]Quartz detected by PXRD and corrected interference calculated from % of quartz found in powder prior to aerosolizing, rather that NIOHH method 7500 analysis of respirable sample.

mineralogical composition. In those cases, the PXRD pattern of the specimen was manually compared to that of the pure mineral reference from the International Center for Diffraction Data's Powder Diffraction File Database (PDF) (Kabekkodu et al. 2024). The criterion for a specimen's inclusion in the study when carrying out the manual comparison was that all peaks in the specimen's diffraction pattern had

to be limited to only those within the intended minerals PDF database diffraction pattern.

Mineral aerosolization and sampling

To evaluate a mineral's interference experimentally, the sample was first prepared as a fine powder specimen which passed a 325-mesh sieve. Grinding was performed when required by way of a diamonite or corundum mortar and pestle. If the powder failed to pass a 325-mesh sieve after grinding by mortar and pestle, it was further wet ground using a micronizing mill (McCrone XRD-Mill 20-077-0001, Westmont, IL, USA) with corundum grinding elements. This method has been recommended (Buhrke et al. 1998) to avoid deleterious effects that can be associated with grinding. The specimen was then analyzed by XRD and aerosolized in a laboratory-based dust chamber. It is worth explicitly stating that the same specimen that was analyzed by XRD after grinding was aerosolized. As a result, any modification or damage during grinding of a sample to produce a specimen for analysis would affect both the determination of the mineral composition by XRD and the acquisition of the FT-IR spectra of the mineral-laden collection filters.

The aerosolized specimens were collected using 10 mm nylon Dorr-Oliver cyclone respirable samplers equipped with three-piece cassettes and pre-weighed GLA-5000 PVC filters with a 5 μm pore size (SKC part no. 225–803). Five parallel respirable samplers collected the aerosol from within a quiescence chamber. The respirable samplers were fitted to a multi-port manifold, with each port having a 1.7 L/min critical orifice. A vacuum was supplied to the manifold and maintained at >190 in H_2O to ensure critical flow through the orifices. The cyclones, which have a 50% cut point of 4 μm when operated at 1.7 L/min, were used to ensure the collected respirable samples were representative of respirable mine dust. This size cut also helped reduce particle size-related effects that could otherwise impact the infrared spectra (Bhaskar et al. 1994).

Five respirable filter samples were generated for each mineral with mass loadings ranging from 50 to 2000 μg. The loadings were determined gravimetrically by way of a 7-place balance (XP2U model, Mettler-Toledo, Columbus, OH, USA) according to the procedure described in the NIOSH Method 600 Particulates not Otherwise Regulated, Respirable.

Analysis of infrared spectra

The infrared spectra of the respirable filter samples were measured in transmission mode with a Bruker (ALPHA model, Bruker Optics, Billerica, MA, USA) using a spectral resolution of 4 cm^{-1} and 3-term Blackman-Harris apodization. A clean GLA-5000 PVC filter was used for background correction. Each spectrum was then integrated across the silica doublet, with the lower limit of the integrated area being defined by a straight line drawn between the absorbances at 816 and 767 cm^{-1}, as previously described (Miller et al. 2012; Ashley et al. 2020; Chubb and Cauda 2022) and shown in Figure 1. The same procedure was applied to a set of five α-quartz reference respirable samples. In this study, Minusil powder (>99% SiO_2 and approximately 89% crystalline α-quartz) (Stacey et al. 2009) was used as the reference material (Figure 2).

The slopes of the integrated doublet area, as illustrated in Figure 2, *vs.* the mineral mass curve for the studied minerals varied based on their relative absorbance within the α-quartz doublet region. The ratio of this slope to that of the reference α-quartz material yielded the *interference percentage* after scaling by a factor of 100. An interference percentage of 100 indicates that the mineral, if quantified solely by integrating the α-quartz doublet, would appear to be 100% α-quartz. The slopes were obtained by way of a linear regression model developed using the *fitlm* function in MATLAB Version 23.2.0.2459199 (Matlab R2023b Update 5, Natick, MA, USA). The slopes so derived were considered valid interfering minerals only if the null hypothesis was rejected at a significance level of $p < 0.05$; otherwise, the mineral's interference was deemed not statistically significant. A regression was also done on baseline absorbance with increasing mineral mass.

Results

The interference percentage, PXRD and NIOSH Method 7500 data, are provided in Table 3. Among the 43 minerals analyzed, 20 were found to have a statistically significant interference. Due to the inability to obtain all minerals in a pure form without α-quartz, the criteria for defining what constituted a high-impact interferant required both statistical significance and consideration of the magnitude of the α-quartz corrected interference percentage. The NIOSH criterion requires that 95% of the samples quantified by an acceptable method be within ± 25% of the true value (Kennedy et al. 1995). Given that this study examined a single component of several which could contribute to the lack of accuracy in an infrared method for quantifying RCS, a threshold of

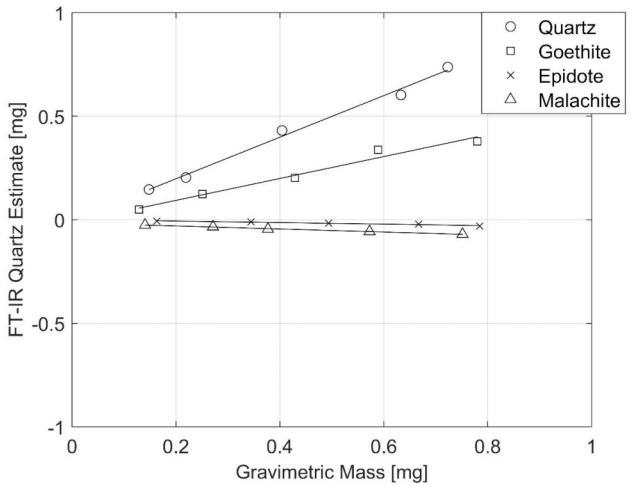

Figure 2. Example of relative absorbance for selected minerals that display interference. The solid lines are the fit of the data to a linear regression.

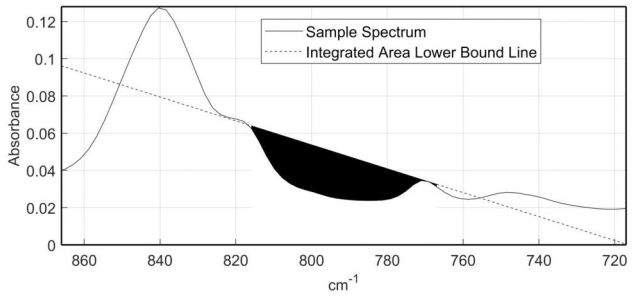

Figure 3. Negative area of an azurite sample as a result of strong absorbance band near the limits of the integrated area.

10% was adopted here. Of the 20 statistically significant mineral specimens, only five showed the potential to interfere by ±10% or greater after correcting for α-quartz content when present. These minerals are referred to as "high-impact interferents" for the sake of brevity and are underlined in Table 3, and their spectra in the doublet region are included in the supplemental material.

Three of the five high-ranking interferents displayed a negative interference. This was caused by prominent absorbance bands near the limits of integration, which pull one or both of the endpoints of the limits of integration up to such an extent that the baseline absorbance between the limits of integration had significant curvature. This curvature resulted in a negative integrated area, as illustrated in Figure 3. The other minerals having statistically significant negative interference (Epidote, Microcline, and Grossular) also had strong absorbance bands near the limits of integration, resulting in similar absorbance baseline behavior and negative integrated area.

The high-ranking interferents goethite (an oxide) and azurite (a carbonate) indicate that a focus on silicates alone is insufficient. Goethite showed the largest interference percentage and was found to be among the most commonly occurring minerals in the mines studied. The previously published interferents listed in Table 4 are all silicates of one form or another, such as phyllosilicates, tectosilicates, etc., except for adamite, which is a hydroxide.

Of the previously published interferants (Ojima 2003; HSE 2005; NIOSH 2017a, 2017b; ISO 2021), all were found to be statistically significant interferants except for albite and anorthite. Montmorillonite was found to be a statistically significant interferent with an interference of 5% and thus could be considered to be confirmed, although it does not meet the 10% criteria to qualify as a "high impact interferent." The lack of significant interference on the part of albite was due to offsetting negative and positive areas, as can be seen in Figure 4 and the supplemental material. The anorthite peaks listed in both databases are outside the limits of integration, and they seem to have a negligible impact on the integrated area. This is a significant result given feldspars are the most common group of minerals in the earth's crust (Neuendorf et al. 2005) and are often mentioned as interferants (Ojima 2003; HSE 2005; NIOSH 2017a, 2017b; ISO 2021).

The only non-mineral sample analyzed, diesel particulate matter (DPM), did not interfere with the doublet integrated area but had a very prominent (greater than any mineral studied) impact on the baseline absorbance. The baseline increased by nearly 1 absorbance unit per mg of DPM on the collection filter, which could result in non-linearity in FT-IR based spectrometry (Griffiths and De Haseth 2007) or could prevented measurement of the α-quartz doublet when using alternative infrared methods. This was further investigated by placing a respirable filter sample with 427 μg of DPM onto the FT-IR beam path in tandem with the standard α-quartz respirable filter samples. The resulting spectra of the tandem DPM and α-quartz respirable filter samples were analyzed for RCS, as described above in the methods section. Regression was performed between the integrated areas with (dependent variable) and without (independent variable) the DPM in tandem, and it was found that the slope of the regression curve was 0.96 with a coefficient of determination was 0.99, indicating little if any divergence from linearity for this amount of DPM in practice.

The NIOSH method 7500 data can be compared to the PXRD data to investigate the anecdotal observation that the percentage of α-quartz in bulk samples

Table 4. List of previously published FT-IR-based quantification of RCS interferents including those evaluated in this study.

	NIOSH 7602 & 7603	HSE MDHS 101/2	Ojima 2003	ISO 24095:2021	Confirmed or Added to List
Adamite			✓		Not analyzed
Albite	✓	✓	✓	✓	Not confirmed
Amorphous silica	✓		✓	✓	Not analyzed
Anorthite	✓	✓		✓	Not confirmed
Anthrophyllite			✓		Not analyzed
Cristobalite	✓	✓		✓	Not analyzed
Daphnite	✓		✓		Not analyzed
Dickite				✓	Not analyzed
Gedrite			✓		Not analyzed
Kaolinite	✓	✓	✓	✓	Confirmed (10%)
Montmorillonite	✓		✓		Confirmed (5%)
Mullite	✓		✓		Not analyzed
Muscovite	✓	✓	✓	✓	Confirmed (−2%)
Orthoclase	✓	✓	✓	✓	Not analyzed
Pyrophyllite	✓		✓		Not analyzed
Talc	✓		✓		Confirmed
Tridymite	✓	✓			Not analyzed
Vermiculite	✓		✓		Not analyzed
Azurite					Added to List
Actinolite					Added to List
Goethite					Added to List
Microcline					Confirmed (−14%)

Checkmarks indicate that the method, standard, or scientific publication listed the given mineral as an interferant.

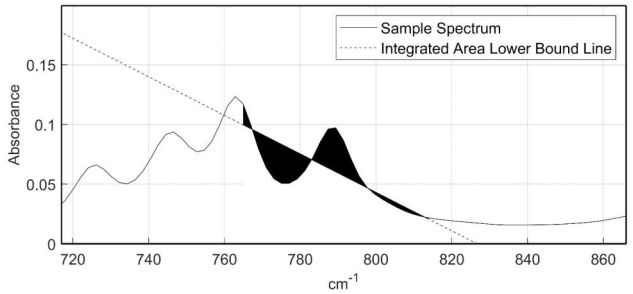

Figure 4. Offsetting areas of an albite sample resulting in insignificant interference in spite of absorbance bands in and near the doublet region.

often exceeds that found in the airborne respirable fraction generated from the same sample (Colinet and Listak 2012; Schatzel 2009). This trend was indeed observed in the current study, as shown in Table 3.

Discussion

This study reviewed 27 metal mines containing a total of 193 distinct minerals according to USGS and Mindat.org. Databases were queried to estimate the potential of these minerals to interfere with RCS quantification via the infrared absorbance doublet. It was not feasible to analyze all 193 minerals in their pure form, and 59 of these did not have spectra available in the databases. Of the 193 minerals, 43 samples that were intended to represent the mineral in question in pure form were obtained. These mineralogical samples were analyzed. The analysis involved generating respirable samples, which were then analyzed using the approach commonly employed for RCS quantification by FT-IR spectrometry. This provided a quantitative assessment of the extent to which each mineral interferes with RCS quantification via the α-quartz doublet. These findings may also be of interest when developing methods to quantify α-quartz by way of alternative infrared absorbance-based techniques, such as quantum cascade laser spectroscopy or non-dispersive infrared spectroscopy.

Results from this analysis support existing literature on the need for correction methods when performing quantification of RCS by way of infrared methods and provide essential data on minerals with the potential to interfere in a subset of US metal mines. The data in this study have expanded the list of known interferants identified in previous works and standards (Ojima 2003; HSE 2005; NIOSH 2017a, 2017b; ISO 2021) by having identified three previously undocumented interferents, goethite, azurite, and actinolite, as shown in Tables 3 and 4. Three of the five high-ranking interferents had negative interference percentages attributed to strong absorbance bands near the limits of the integrated area. The feldspars albite and anorthite are conspicuously not included in the list of high-ranking mineral interferents. The lack of high-ranking interference on the part of these feldspars is significant, given the ubiquitousness of this mineral group in the earth's crust and the fact that they are listed as interferents in the methods and standards (HSE 2005; NIOSH 2017a, 2017b; ISO 2021).

A critical step toward implementing interferent corrections is to identify which potentially interfering minerals are present. The spectra of these interfering minerals can then be used to implement interferent correction methods such as area ratio correction,

spectral subtraction, or multivariate/chemometric modeling.

A limitation of area ratio correction and spectral subtraction methods is that they rely on the existence of an additional "spectrally pure" absorbance band in the interferant's spectrum that is isolated from the bands of any other mineral within the sample. Both these approaches aim to eliminate the influence of interferants on the spectrum and produce a spectral response that is due only to that of the α-quartz in the sample. In contrast, multivariate calibration does not require the regions used to estimate α-quartz to be only affected by the mass of α-quartz, but rather requires that the target analyte's spectrum be at least partially distinct from those of all other contributing species (Kalivas and Gemperline 2006). Fortunately, as noted by Povarennykh (Povarennykh 1978), "in practice, in no case do we encounter minerals with completely identical absorption spectra."

Multivariate regression techniques commonly applied to spectra manipulate Beer's law to form a model with either the concentrations (p-matrix) or spectra (k-matrix) as the dependent variable (Kalivas and Lang 1994; Griffiths and De Haseth 2007). The advantage of the p-matrix formulation is that it allows for calibration when the concentration of *only* the target analyte is known, while the concentrations of interfering species are unknown. In contrast, the k-matrix approach requires knowledge of the concentrations of both the analyte of interest and that of any interfering species. While this makes the p-matrix approach appealing, applying it in its basic form requires that the number of calibration spectra be at least equal to or greater than the number of wavenumbers sampled in each spectrum (Strang 2003). A typical transmission FT-IR spectrum includes many absorbance measurements across the mid-infrared range, for example, the spectra in Figure 5 contain 1,764 data points each. In practice, this implies a reduction in the number of wavenumbers in the spectrum to only those that are relevant. Further, the wavenumbers selected should be independent to allow for the necessary matrix inversion (or pseudoinversion) solution to Beer's law, an issue sometimes referred to as the spectral collinearity problem (Næs and Mevik 2001; Kalivas and Gemperline 2006; Otto 2024). This last requirement is difficult to ensure without extensive knowledge of all the interfering mineral spectra. Fortunately, biased regression techniques, such as partial least squares (PLS) regression and principal component regression (PCR), offer effective solutions to this problem. In this context,

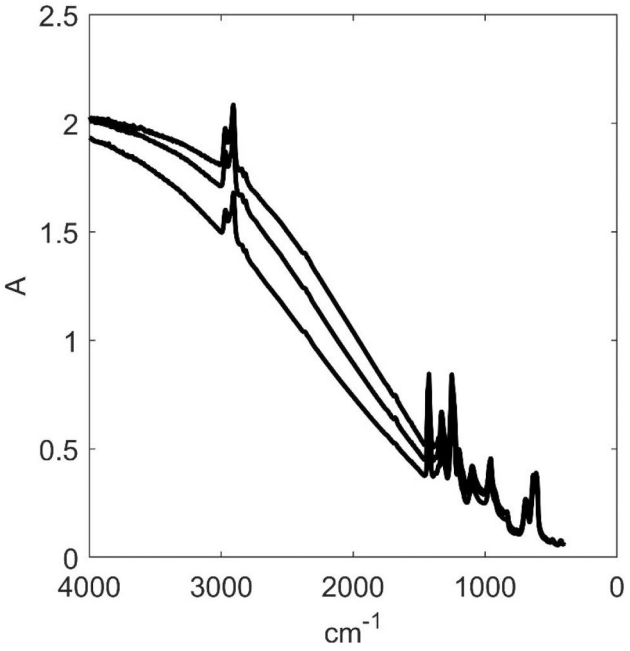

Figure 5. Spectra of 3 clean 5 μm pore size PVC filters.

bias refers to allowing bias, ideally while reducing variance, in the determination of the model coefficients and does not imply bias in the quantification of the analyte (Kalivas and Lang 1994; Faber 1999). Various studies have shown the promise of such chemometric techniques when applied to the FT-IR spectra of respirable quartz samples, including (Salehi et al. 2021; Stacey et al. 2022; Wolfe et al. 2022). These biased regression techniques enable implementation when (1) the sample is composed of multiple minerals/analytes with overlapping infrared absorbance bands, (2) the concentration of *only* the target analyte is known, (3) fewer calibration spectra than wavenumbers within each spectrum are available, and (4) wavenumbers sampled are not independent. These features make the multivariate chemometric approaches the most promising when striving for a single method for processing infrared spectra to quantify α-quartz from a diverse range of samples spanning all mining commodities.

To implement these biased regression techniques, calibration samples need to be collected that include all potentially present interfering minerals—as well as RCS—at concentrations that span the full range expected in future analyses. This requirement ensures that the model does not extrapolate outside the calibrated range; however, extrapolation may be valid if the infrared response remains linear at concentrations outside those included in the calibration (Griffiths and De Haseth 2007). It may not always be possible to ensure that no analyte exceeds the calibrated range;

however, a sample with an analyte that does would likely produce a spectrum distinguishable by PCA and could be flagged as an outlier. This outlier could then be further analyzed—e.g., via NIOSH Method 7500—and incorporated into the calibration set, thereby expanding the model's applicable range (Wolfe et al. 2022).

Limitations

The RCS quantification approach investigated in this study is relatively simple, in that it focuses on a single region of the infrared (IR) spectrum. Further, it is well known that using multiple absorbance bands often enhances both sensitivity and selectivity of FT-IR-based quantification methods (Griffiths and De Haseth 2007; Olivieri 2008). Despite its simplicity, the method examined here aligns with those described in widely accepted analytical protocols (NIOSH 2017a, 2017b) and is currently employed by regulatory agencies in the US and Britain, including the HSE and MSHA (HSE 2005; MSHA 2014).

Much of the utility of the results presented in this study is contingent upon the validity of the assumption of linear superposition of spectra. The assumption of linear superposition may not always be met for respirable particulate on collection filter samples. However, this assumption is implicitly assumed in the interferent correction approaches implemented in widely accepted analytical protocols (NIOSH 2017a, 2017b) and by regulatory agencies (HSE 2005; MSHA 2014).

Provided linear superposition of spectra can be assumed, the percent interference listed in Table 3 can be summed to provide an estimate of the result of the doublet integration method applied to a sample composed of a mixture of minerals. For example, a sample containing 100 μg of α quartz and 100 μg of azurite would appear to be composed of 76 μg of α-quartz due to the −24% interference of azurite. Specifically, the quartz corrected interference within Table 3 would be used to arrive at such an estimate.

Many of the minerals studied had multiple corresponding spectra available in the databases. In several cases, the spectra for a single mineral differed, even within the same database, highlighting the need for further corroboration or refutation of the mineral's potential to interfere. The peak locations for all the minerals investigated are provided in the supplemental material. The inconsistent database spectra may be due to several factors including the allowance of substitutional elements diverging from the IMA-accepted stoichiometry and the fact that some IMA-accepted minerals are actually solid solutions (see supplemental information). Additionally, when preparing a powdered mineral specimen, in spite of all efforts, there will always be some lack of reproducibility or even repeatability in multiple specimens prepared from a single source material.

Conclusion

Of the 43 minerals analyzed, 17 showed statistically significant potential to interfere with the quantification of RCS by infrared absorbance measurement of the α-quartz doublet absorbance bands. Only five minerals were deemed "high ranking interferents" based on their potential to interfere with a magnitude of 10% or more. Three of these five minerals had not previously been reported as interferents in the literature. All five of these minerals were suspected of interference, prior to laboratory analysis, based on the spectra databases queried. However, 10 minerals were similarly suspect based on the database spectra but were found to display interference of less than 10%. This indicates that spectral databases are of limited use for determining the magnitude of interference; all confounding minerals were suspected, but not all suspected minerals were confounders. None of the feldspar specimens showed the potential to interfere with a magnitude of 10% or greater. This last result is noteworthy given that feldspars are the most common group of minerals in the earth's crust and are often mentioned as interferents in the context of quantifying RCS both by FT-IR *and* XRD. Feldspars are silicates with known bands in the doublet region; however, the particular way the doublet region is integrated in this study results in offsetting positive and negative contributions to the integrated area (as shown in Figure 4).

The more geologically diverse mineral content in metal and nonmetal mines compared to coal mines has led MSHA to require X-ray diffraction (XRD) for RCS quantification in those settings (MSHA 2024a). Nevertheless, infrared absorbance instrumentation is significantly more affordable and portable, making it a promising candidate for real-time or end-of-shift field-based monitoring, provided that correction for mineral interferants can be implemented.

Ideally, the data collected in this study, which include the concentrations of all analytes, would be used to develop a calibration for a portable infrared RCS monitor. The procedure carried out in this study could be repeated for all the known α-quartz

absorbance bands, e.g., at roughly 1171, 1145, 1084, 696, 513, and 459 $cm^{-1,}$ which could reduce the number of high-ranking interferents. The data herein, which include concentrations of *all* analytes, could be used to develop either p-matrix or k-matrix type calibrations. This calibration could then be used to aid in the development of a low-resolution infrared device for quantifying RCS that is portable and has no moving parts, similar to a non-dispersive infrared spectrometer developed for DPM (Parks et al. 2024). Such a monitor could be made wearable. On the other hand, a biased regression technique applied to FT-IR spectra will be more adaptable and accurate, though the current state of midinfrared FT-IR technology is not compatible with a wearable device unless a means of presenting the sample amenable to attenuated total reflectance mode is devised.

Disclaimer

The findings and conclusions in this report are those of the author and do not necessarily represent the official position of the National Institute for Occupational Safety and Health (NIOSH), Centers for Disease Control and Prevention (CDC). Mention of any company or product does not constitute endorsement by NIOSH, CDC.

Disclosure statement

No potential conflict of interest was reported by the author(s).

Data availability statement

The data that support the findings of this study are available from the corresponding author, upon reasonable request.

References

Ainsworth SM. 2005. Infrared analysis of respirable coal mine dust for quartz: thirty-five years. J ASTM Int. 2(4): 1–13. https://doi.org/10.1520/JAI12231

Ashley EL, Cauda E, Chubb LG, Tuchman DP, Rubinstein EN. 2020. Performance comparison of four portable FTIR instruments for direct-on-filter measurement of respirable crystalline silica. Ann Work Expo Health. 64(5): 536–546. https://doi.org/10.1093/annweh/wxaa031

Barnes H, Goh NS, Leong TL, Hoy R. 2019. Silica-associated lung disease: an old-world exposure in modern industries. Respirology. 24(12):1165–1175. https://doi.org/10.1111/resp.13695

Barnes RJ, Dhanoa MS, Lister SJ. 1989. Standard normal variate transformation and de-trending of near-infrared diffuse reflectance spectra. Appl Spectrosc. 43(5):772–777. https://doi.org/10.1366/0003702894202201

Bhaskar R, Li J, Xu L. 1994. A comparative study of particle size dependency of IR and XRD methods for quartz analysis. Am Ind Hyg Assoc J. 55(7):605–609. https://doi.org/10.1080/15428119491018682

Buhrke VE, Jenkins R, Smith DK. 1998. General introduction. In: Buhrke VE, Jenkins R, Smith DK, editors. A practical guide for the preparation of specimens for X-ray fluorescence and X-ray diffraction analysis. John Wiley & Sons. p. 23–24.

Chubb LG, Cauda EG. 2022. Direct-on-filter analysis for respirable crystalline silica using a portable FTIR instrument. Information Circular 9533. Cincinnati (OH): U.S. Department of Health and Human Services, Centers for Disease Control and Prevention, National Institute for Occupational Safety and Health, DHHS (NIOSH) Publication No. 2022-108. https://www.cdc.gov/niosh/mining/works/coversheet2175.html

Chukanov NV. 2014. Infrared spectra of mineral species: extended library. Springer Science & Business Media.

Colinet JF, Listak JM. 2012 Dec 20. Silica and respirable content in rock dust samples. Coal Age; [accessed 2025 Jun 20]. https://wwwcoalagecom/flipbooks/december-2012/

Ehrlich R, Akugizibwe P, Siegfried N, Rees D. 2021. The association between silica exposure, silicosis and tuberculosis: a systematic review and meta-analysis. BMC Public Health. 21(1):953. https://doi.org/10.1186/s12889-021-10711-1

Faber NM. 1999. A closer look at the bias–variance tradeoff in multivariate calibration. J Chemometrics. 13(2): 185–192. https://doi.org/10.1002/(SICI)1099-128X(199903/04)13:2<185::AID-CEM538>3.0.CO;2-N

Griffiths PR, De Haseth JA. 2007. Fourier transform infrared spectrometry. 2nd ed. John Wiley & Sons.

HSE. 2005. MDHS 101/2 crystalline silica in respirable airborne dusts-direct-on-filter analysis by infrared spectroscopy and X-ray diffraction. Health and Safety Excecutive (HSE).

IARC. 1997. Working group on the evaluation of carcinogenic risks to humans. Silica, some silicates, coal dust and para-aramid fibrils. IARC Monographs on the Evaluation of Carcinogenic Risks to Humans, No. 68. Silica. https://www.ncbi.nlm.nih.gov/books/NBK410038/

ISO. 2021. 24095 Workplace air – guidance for the measurement of respirable crystalline silica. International Organization for Standardization.

Kabekkodu SN, Dosen A, Blanton TN. 2024. 5+: a comprehensive powder diffraction file for materials characterization. Powder Diffr. 39(2):47–59. https://doi.org/10.1017/S0885715624000150

Kaduk JA. 2008. Structure refinement. In: Clearfield A, Reibenspies JH, Bhuvanesh N, editors. Principles and applications of powder diffraction. John Wiley & Sons. p. 310–361.

Kalivas JH, Gemperline PJ. 2006. Calibration. In: Gemperline PJ, editor. Practical guide to chemometrics. 2nd ed. CRC/Taylor & Francis. p. 105–166.

Kalivas JH, Lang PM. 1994. Mathematical analysis of spectral orthogonality. Marcel Dekker.

Kennedy ER, Fischbach TJ, Song R, Eller PM, Shulman SA. 1995. Guidelines for air sampling and analytical method development and evaluation. National Institute for Occupational Safety and Health. Report No: 95-117.

Lafuente B, Downs RT, Yang H, Stone N. 2015. The power of databases: the RRUFF project. In: Armbruster T, Danisi RM, editors. Highlights in mineralogical crystallography. Walter de Gruyter GmbH. p. 1–30.

Leung CC, Yu ITS, Chen W. 2012. Silicosis. Lancet. 379(9830):2008–2018. https://doi.org/10.1016/s0140-6736(12) 60235-9

Martínez C et al. 2010. Silicosis: a disease with an active present. Archiv Bronconeumol (English Ed). 46(2):97–100. https://doi.org/10.1016/S1579-2129(10)70022-7

Miller AL, Drake PL, Murphy NC, Noll JD, Volkwein JC. 2012. Evaluating portable infrared spectrometers for measuring the silica content of coal dust. J Environ Monit. 14(1):48–55. https://doi.org/10.1039/c1em10678c

Miller AL, Weakley AT, Griffiths PR, Cauda EG, Bayman S. 2017. Direct-on-filter α-quartz estimation in respirable coal mine dust using transmission Fourier transform infrared spectrometry and partial least squares regression. Appl Spectrosc. 71(5):1014–1024. https://doi.org/10.1177/0003702816666288

Misra S, Sussell AL, Wilson SE, Poplin GS. 2023. Occupational exposure to respirable crystalline silica among US metal and nonmetal miners, 2000–2019. Am J Ind Med. 66(3):199–212. https://doi.org/10.1002/ajim.23451

MSHA. 2014. MSHA P-7: infrared spectroscopy determination of quartz in respirable coal mine dust. Washington (DC): Department of Labor Mine Safety and Health Administration Technical Support Pittsburgh Safety and Health Technology Center; [accessed 2025 Jul 8]. https://www.msha.gov/sites/default/files/Support_Resources/PUBLIC%20FINAL%20New_P7%202024.pdf

MSHA. 2024a. Lowering miners' exposure to respirable crystalline silica and improving respiratory protection. Arlington (VA): Mine Safety and Health Administration (MSHA); [accessed 2024 May 5]. https://www.federalregister.gov/d/2024-06920

MSHA. 2024b. Personal health samples dataset. Arlington (VA): Mine Safety and Health Administration (MSHA); [accessed 2024 June 10]. https://arlweb.msha.gov/OpenGovernmentData/OGIMSHA.asp

Næs T, Mevik BH. 2001. Understanding the collinearity problem in regression and discriminant analysis. J Chemometrics. 15(4):413–426. https://doi.org/10.1002/cem.676

Neuendorf KKE, Mehl JP, Jackson JA. 2005. Glossary of geology. 5th ed. The American Geosciences Institute.

NIOSH. 2017a. Quartz in respirable coal mine dust, by IR (KBr pellet) 7602. NIOSH manual of analytical methods. 5th ed. National Institute for Occupational Safety and Health (NIOSH). Publication No. 2014-151. https://www.cdc.gov/niosh/nmam/pdf/7602.pdf

NIOSH. 2017b. Quartz in respirable coal mine dust, by IR (Redeposition) 7603. NIOSH manual of analytical methods. 5th ed. National Institute for Occupational Safety and Health (NIOSH). Publication No. 2014-151. https://www.cdc.gov/niosh/nmam/pdf/7603.pdf

Ocaña M, Fornes V, García-Ramos JV, Serna CJ. 1987. Polarization effects in the infrared spectra of α-quartz and α-cristobalite. Phys Chem Miner. 14:527–532. https://doi.org/10.1007/BF00308288

Ojima J. 2003. Determining of crystalline silica in respirable dust samples by infrared spectrophotometry in the presence of interferences. J Occup Health. 45(2):94–103. https://doi.org/10.1539/joh.45.94

Olivieri AC. 2008. Analytical advantages of multivariate data processing. One, two, three, infinity? Anal Chem. 80(15):5713–5720. https://doi.org/10.1021/ac800692c

OSHA/NIOSH. 2012. Hazard alert: worker exposure to silica during hydraulic fracturing. Washington (DC): U.S. Department of Labor, Occupational Safety and Health Administration; [accessed 2025 Jun 23]. https://www.osha.gov/sites/default/files/publications/hydraulic_frac_hazard_alert_0.pdf

Otto M. 2024. Chemometrics: statistics and computer application in analytical chemistry. 4th ed. Wiley-VCH GmbH.

Parks DA, Zhao Y, Griffiths PR, Miller AL. 2024. Evaluation of a non-dispersive infrared spectrometer for quantifying organic and elemental carbon in diesel particulate matter. Aerosol Sci Technol. 58(6):694–705. https://doi.org/10.1080/02786826.2024.2322681

Povarennykh A. 1978. The use of infrared spectra for the determination of minerals. Am Mineral. 63(9-10):956–959.

Rice F et al. 2001. Crystalline silica exposure and lung cancer mortality in diatomaceous earth industry workers: a quantitative risk assessment. Occup Environ Med. 58(1):38–45. https://doi.org/10.1136/oem.58.1.38

Rietveld HM. 1969. A profile refinement method for nuclear and magnetic structures. J Appl Crystallogr. 2(2):65–71. https://doi.org/10.1107/S0021889869006558

Rose C. 2019. Severe silicosis in engineered stone fabrication workers—California, Colorado, Texas, and Washington, 2017–2019. MMWR Morb Mortal Wkly Rep. 68:813–818. https://doi.org/10.15585/mmwr.mm6838a1

Salehi M, Zare A, Taheri A. 2021. Artificial neural networks (ANNs) and partial least squares (PLS) regression in the quantitative analysis of respirable crystalline silica by Fourier-transform infrared spectroscopy (FTIR). Ann Work Expo Health. 65(3):346–357. https://doi.org/10.1093/annweh/wxaa097

Schatzel SJ. 2009. Identifying sources of respirable quartz and silica dust in underground coal mines in southern West Virginia, western Virginia, and eastern Kentucky. Int J Coal Geol. 78(2):110–118. https://doi.org/10.1016/j.coal.2009.01.003

Stacey P, Clegg F, Rhyder G, Sammon C. 2022. Application of a Fourier transform infrared (FTIR) principal component regression (PCR) chemometric method for the quantification of respirable crystalline silica (Quartz), kaolinite, and coal in coal mine dusts from Australia, UK, and South Africa. Ann Work Expo Health. 66(6):781–793. https://doi.org/10.1093/annweh/wxab119

Stacey P et al. 2009. An international comparison of the crystallinity of calibration materials for the analysis of respirable α-quartz using X-ray diffraction and a comparison with results from the infrared KBr disc method.

Ann Occup Hyg. 53(6):639–649. https://doi.org/10.1093/annhyg/mep038

Straif K et al. 2009. A review of human carcinogens-part C: metals, arsenic, dusts, and fibres. Lancet Oncol. 10(5): 453–454. https://doi.org/10.1016/S1470-2045(09)70134-2

Strang G. 2003. Introduction to linear algebra. 3rd ed. Wellesley-Cambridge Press.

Walker RL et al. 2021. Complexity of respirable dust found in mining operations as characterized by X-ray diffraction and FTIR analysis. Minerals. 11(4):383. https://doi.org/10.3390/min11040383

Weakley AT, Miller AL, Griffiths PR, Bayman SJ. 2014. Quantifying silica in filter-deposited mine dusts using infrared spectra and partial least squares regression. Anal Bioanal Chem. 406(19):4715–4724. https://doi.org/10.1007/s00216-014-7856-y

Weissman D, Schulte P. 2011. The continuing persistence of silicosis. [blog]. NIOSH Science Blog; [accessed 2025 Jun 22]. https://blogs.cdc.gov/niosh-science-blog/2011/10/18/silicosis/

Wolfe C, Chubb L, Walker R, Yekich M, Cauda E. 2022. Monitoring worker exposure to respirable crystalline silica: application for data-driven predictive modeling for end-of-shift exposure assessment. Ann Work Expo Health. 66(8):1010–1021. https://doi.org/10.1093/annweh/wxac040